

Electric monopole admixtures in interband transitions of $^{154}\text{Gd}^\dagger$

Y. Gono and T. T. Sugihara

Cyclotron Institute, Texas A & M University, College Station, Texas 77843

(Received 26 August 1974)

The in-beam conversion-electron spectrum for the reaction $^{154}\text{Sm}(\alpha, 4n)^{154}\text{Gd}$ has been obtained at 45 MeV. Strong $E0$ components are observed for interband transitions between states in the β and ground bands up to at least spin 10 and probably also spin 12. The ratio of transition probabilities, $E0$ to $E2$, is found to be essentially constant for I_β in the range 2 to 10. No evidence for a dramatic change which might be associated with the backbending phenomenon is seen.

NUCLEAR REACTIONS $^{154}\text{Sm}(\alpha, 4n)$, $E = 45$ MeV, enriched target; measured in-beam I_{ce} , I_γ . ^{154}Gd deduced ICC, $B(E0)/B(E2)$.

I. INTRODUCTION

A rapid increase of the moment of inertia, the phenomenon called backbending, has been observed at high spin in the ground-state rotational bands of many rare-earth nuclei.^{1,2} Subsequently, similar anomalous changes in the moments of inertia were found in the β -vibrational bands of ^{154}Gd (Refs. 3 and 4) and ^{156}Dy (Refs. 5 and 6). Backbending has been attributed to the Coriolis antipairing (CAP) effect^{7,8} or the crossing of bands^{9,10} which have different moments of inertia.

In the case of ^{154}Gd , Khoo *et al.*⁴ showed that an excited band (presumably the β band) crossed the ground band, and they attribute the backbending observed in the yrast sequence to the band crossing. They speculate that the backbending in the β band may also be the result of a band crossing. In fact, they suggest⁴ that backbending in both bands might be interpreted in terms of a third band which intersects the β band to become the "yrare" sequence [an yrare level, in the terminology of Ref. 4, is the first excited state above the lowest (yrast) state of the same spin] for $I \geq 12$ and further intersects the ground band to form the yrast levels for $I \geq 18$. If the intersecting band is dominated by $K \neq 0$, the monopole matrix element between β -band states and ground-band states might undergo a substantial reduction in the band crossing region.

If backbending is a CAP effect, the monopole matrix element should also be strongly affected. For a pairing phase transition, Kumar has predicted¹¹ that the ratio of $E0$ to $E2$ transition probabilities should increase strongly.

The determination of $E0$ matrix elements for higher-spin states in ^{154}Gd thus appeared to be an interesting approach to the study of backbending. Previous work on $E0$ transitions in ^{154}Gd includes low-spin data from the radioactive decay of ^{154}Eu in which the mixing of $E0$, $M1$, and $E2$ components

in transitions between β -band and ground-band states has been analyzed.^{12,13} In-beam electron spectra¹⁴ have been reported for the $^{152}\text{Sm}(\alpha, 2n)^{154}\text{Gd}$ reaction and $E0$ components of interband transitions have been observed up to $I = 8$. Unfortunately this work was done before the era of high-resolution γ -ray detectors and detailed γ -ray information was not available. In a more recent experiment involving in-beam γ rays,¹⁵ angular distributions were obtained and $E2/M1$ mixing was deduced. No conversion-electron information was obtained, however. By a lifetime measurement of the 0^+_β state in ^{154}Gd , together with earlier data,¹² Rud *et al.*¹⁶ were able to show that the reduced $E0$ matrix element in ^{154}Gd was independent of spin up to spin 6.

In this paper we report the results of a study of the $^{154}\text{Sm}(\alpha, 4n)^{154}\text{Gd}$ reaction in which the prompt deexcitation of ^{154}Gd was observed with both γ -ray and electron detectors. Electron data are reported to spin 10 with qualitative information about spin 12.

II. EXPERIMENTAL METHODS

A conversion-electron spectrometer which transports electrons in trochoidal orbits was used in this work. A cross section of the spectrometer, as viewed perpendicular to the beam direction, is shown schematically in Fig. 1. The conversion electrons emitted from a target drift to the detector position following a trochoidal orbit in a fringing magnetic field which is generated by a pair of circular pole tips. Positrons go in the opposite direction around the pole tips. The detector is well shielded from γ rays and other particles by 25.4 cm of lead which is put between the two magnet pole faces. The general principles on which the device is based have been described elsewhere.^{17,18}

An instrument of this type has relatively high transmission but provides essentially no energy resolution. The analysis of electron energies is

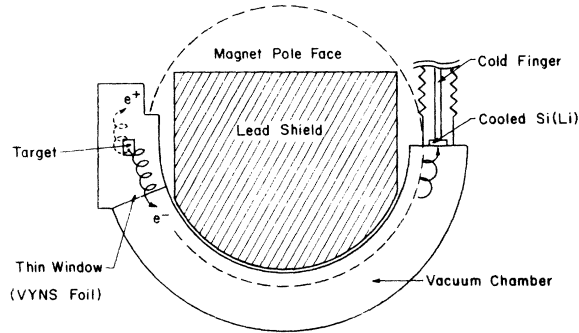


FIG. 1. Schematic cross sectional view of in-beam conversion-electron spectrometer.

carried out by a cooled Si(Li) detector. To maintain optimum resolution, the detector is kept in a clean vacuum separated from the beam-line vacuum by a VYNS window $30 \mu\text{g}/\text{cm}^2$ thick. The window serves to remove some of the low-energy background electrons as well.

A relative efficiency curve for the system is shown in Fig. 2. This was determined with radioactive sources; the data shown are for ^{75}Se (Ref. 19) and $^{205,206,207}\text{Bi}$ (Ref. 20). These points were taken with a magnet current of 60 A which generates 3.0 kG at the average radius of the electron orbit. This current setting is useful for transmitting electrons with energies between 0.2 and 1 MeV. Details of the spectrometer system will be reported elsewhere.²¹

A self-supporting foil of Sm ($0.8 \text{ mg}/\text{cm}^2$ and enriched to 98.7% in ^{154}Sm) was bombarded with 45-MeV α particles from the Texas A & M variable energy cyclotron. A portion of the electron spectrum, taken for 60 min with a 40-nA beam, is shown in Fig. 3. The γ -ray spectrum taken with a Ge(Li) detector under similar bombarding conditions is also shown. In the latter case, a $10\text{-mg}/\text{cm}^2$ metal target was used. Both spectra were taken at 90° to the beam axis. The horizontal scale in Fig. 3 was adjusted so that a γ -ray line and its K -converted electron line have the same peak position.

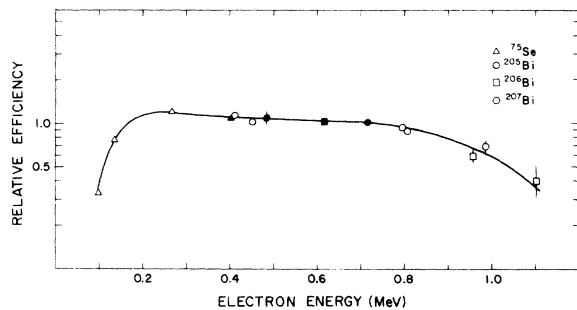


FIG. 2. Relative efficiency of electron spectrometer. Closed symbols indicate normalization points.

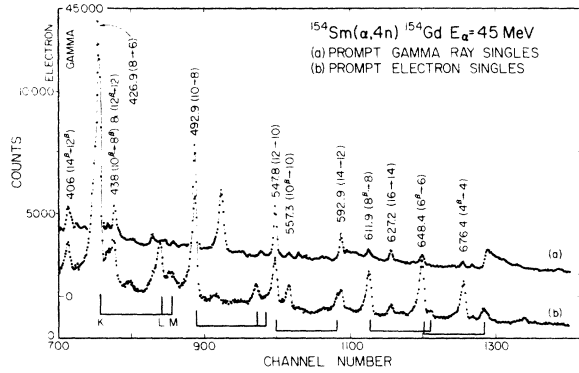


FIG. 3. In-beam γ -ray (a) and conversion-electron (b) spectra from the $^{154}\text{Sm}(\alpha, 4n)^{154}\text{Gd}$ reaction at 45 MeV. The horizontal energy scale has been displaced so that a γ -ray peak and its corresponding K -converted electron line are superimposed.

III. RESULTS

The ground-state band and β -vibrational band of ^{154}Gd have been established to $I^\pi = 18^+$. The level scheme of Khoo *et al.*⁴ is shown in Fig. 4. We drop the parity label in what follows since all the states involved have positive parity. The subscript β is used to identify states in the β band; unsubscripted I values refer to ground-band states.

Relative intensities of γ rays of importance to this study and of their corresponding K -converted electrons are listed in Table I. The two intensity scales were normalized by requiring the 346.5-keV 6-4 transition to have an internal conversion coefficient (ICC) corresponding to pure $E2$.²²

The intensities of both γ rays and electrons have been corrected for their angular distributions. In the case of γ rays, the correction factor η_γ was calculated from the equation

$$\eta_\gamma = \left[\int_{\theta_1}^{\theta_2} W_\gamma(\theta) \sin\theta d\theta \right] / \left(A_0 \int_{\theta_1}^{\theta_2} \sin\theta d\theta \right). \quad (1)$$

Here, the angular-distribution function $W_\gamma(\theta)$ was taken to be

$$W_\gamma(\theta) = A_0 \left[1 + (A_2/A_0)P_2(\cos\theta) + (A_4/A_0)P_4(\cos\theta) \right]. \quad (2)$$

Experimental values of A_2/A_0 and A_4/A_0 reported for the $^{154}\text{Sm}(\alpha, 4n)^{154}\text{Gd}$ reaction at 41 MeV were used.³ The angles θ_1 and θ_2 in Eq. (1) are 90° and 90° plus 19.7° , respectively; 19.7° is one-half the angle subtended by the Ge(Li) detector at the target.

For internally converted transitions between members of the ground-state band, the correction η_e was obtained from an equation similar to E (1). The angular-distribution function was given by

$$W_e(\theta) = A_0 [1 + b_2(A_2/A_0)P_2(\cos\theta) + b_4(A_4/A_0)P_4(\cos\theta)] \quad (3)$$

The values of the particle parameters b_i were taken from Hager and Seltzer.²³ The integration limits θ_1 and θ_2 for the electron case are 90° and $90^\circ + \psi/2$, respectively, where ψ is the acceptance angle for electrons emitted by the target. For the trochoidal system used in this work, ψ is obtained from²⁴

$$\sin\psi = \frac{nh}{2d\sqrt{2}} \quad (4)$$

Here d is the distance between the target position and the magnet center (17.15 cm), h is the width of the vacuum chamber (3.49 cm) between the pole tips, and n is the magnetic field constant (4.60). Thus, ψ is found to be 19.3° .

In the case of $\Delta I = 0$ transitions between members of the β band and the ground-state band, the conversion-electron spectrum was dominated by the $E0$ component (>60% up to $I = 10$). Thus, for these

transitions the electron angular distribution was assumed to be isotropic. The error introduced by this assumption is at most 4%.

Conversion coefficients obtained from these data are shown in Fig. 5. Transitions between members of the ground-state band fall as expected on the theoretical curve for $E2$ transitions. The data point for the $14 \rightarrow 12$ transition is not included since the K -converted peak in the electron spectrum is obscured by the L -converted lines of the $12 \rightarrow 10$ transition. For the other transitions in Fig. 5, the ICC value [except that labeled $(10_\beta \rightarrow 8_\beta) + (12_\beta \rightarrow 12)$] greatly exceeds that for $M1$. The spins and parities of the deexciting levels are well established.^{3,4} Higher multipoles such as $M3$ and $E4$ cannot compete with interband $E2$ transitions. We conclude that the large ICC values can be accounted for only if there is a large $E0$ component in the interband transitions. The theoretical curves in Fig. 5 assume no penetration effects.²⁵ As in the case of the lower-spin states of ^{154}Gd , this effect is taken to be small.

The $8_\beta \rightarrow 8$ transition energy is nearly the same as that of the $18 \rightarrow 16$ transition. The γ -ray and electron intensities in Table I for the $8_\beta \rightarrow 8$ transition have been corrected for the contributions of the $18 \rightarrow 16$ transition, as deduced from the data given in Ref. 4.

The experimentally determined 438-keV transition is a mixture of the $10_\beta \rightarrow 8_\beta$ and $12_\beta \rightarrow 12$ transitions. We can extract the $10_\beta \rightarrow 8_\beta$ component of the mixture if we assume that the branching of the

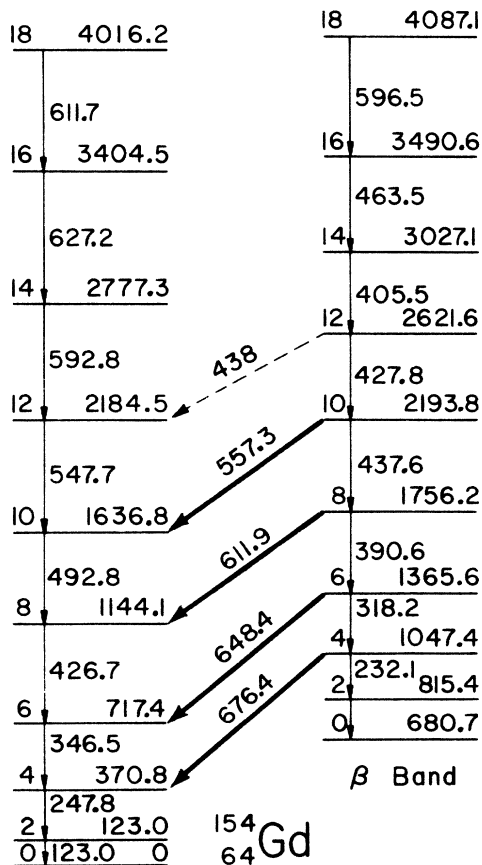


FIG. 4. Level scheme of ^{154}Gd from Ref. 4. Heavy lines indicate interband transitions for which data are reported in this paper.

TABLE I. Relative intensities of γ rays and conversion electrons in the $^{154}\text{Sm}(\alpha, 4n\gamma)^{154}\text{Gd}$ reaction at 45 MeV.

E_γ (keV)	N_γ	N_e^K	α_K (units 10^{-2})	Transition
247.9	113 ± 8	935 ± 87	8.27 ± 1.19	4 → 2
346.5	100 ± 7	306 ± 14	≅ 3.06 ^a	6 → 4
390.6	9.7 ± 0.5	b		$8_\beta \rightarrow 6_\beta$
426.9	83 ± 6	141 ± 9	1.70 ± 0.22	8 → 6
438	13 ± 2	28 ± 5	2.20 ± 0.45	$12_\beta \rightarrow 12$ $10_\beta \rightarrow 8_\beta$
492.9	51 ± 3.5	63 ± 8	1.24 ± 0.21	10 → 8
547.8	28 ± 2	25.4 ± 3.5	0.91 ± 0.16	12 → 10
557.3	2.5 ± 0.4	11.4 ± 2.0	4.6 ± 1.2	$10_\beta \rightarrow 10$
611.9	3.6 ± 0.2 ^c	18.9 ± 2.3 ^c	5.3 ± 0.7	$8_\beta \rightarrow 8$
627.2	7.2 ± 0.5	4.3 ± 1.2	0.6 ± 0.2	16 → 14
648.4	6.7 ± 0.6	26.2 ± 3.2	3.9 ± 0.7	$6_\beta \rightarrow 6$
676.4	4.2 ± 0.3	16.9 ± 2.0	4.0 ± 0.7	$4_\beta \rightarrow 4$

^a Normalized to theoretical value (Ref. 22) for $E2$ transition.

^b The 390.6 K line (340.6 keV) is masked by the strong 346.5 L lines (338.5 keV).

^c Corrected for the contribution from the $18 \rightarrow 16$ transition (data from Ref. 4).

8_β and 10_β levels are the same with respect to interband and intraband transitions. That is, we assume

$$\frac{B(E2, 10_\beta \rightarrow 8_\beta)}{B(E2, 10_\beta \rightarrow 10)} = \frac{B(E2, 8_\beta \rightarrow 6_\beta)}{B(E2, 8_\beta \rightarrow 8)} \quad (5)$$

If the data in Table I are substituted into Eq. (5), the γ -ray intensity of the 438-keV $10_\beta \rightarrow 8_\beta$ transition is found to be 12.9 ± 2.3 units. Since the measured total γ -ray intensity at that energy is 13 ± 2 units, nearly all of the 438-keV γ -ray intensity can be attributed to the $10_\beta \rightarrow 8_\beta$ transition and only a small amount to the $12_\beta \rightarrow 12$ transition.

While we cannot obtain a quantitative value for α_K of the $12_\beta \rightarrow 12$ transition, it is apparent that its value is large compared to that for an $E2$ or $M1$ transition. For example, assume that the γ -ray intensity $N_\gamma(10_\beta \rightarrow 8_\beta)$ is 12 and that $N_\gamma(12_\beta \rightarrow 12)$ is 1; α_K for a 438-keV $E2$ transition is 0.0161. Thus, the electron intensity $N_e(10_\beta \rightarrow 8_\beta)$ is 0.19. The observed intensity $N_e(438 \text{ keV})$ is 0.28 ± 0.05 and $N_e(12_\beta \rightarrow 12)$ is then 0.09 ± 0.05 . This leads to an effective α_K value of 0.09 ± 0.05 for the

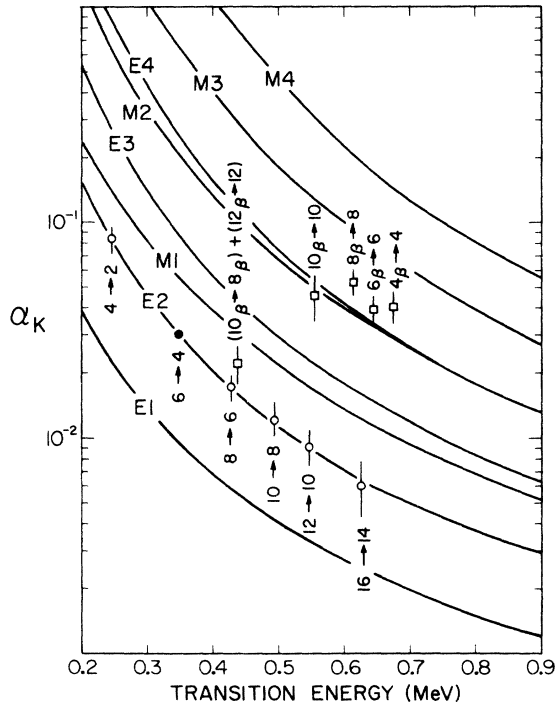


FIG. 5. Internal-conversion coefficients for ground-band transitions (circles) and $\Delta I = 0$ transitions between β -band and ground-band states (squares). The electron and γ -ray intensity scales were normalized such that α_K for the $6 \rightarrow 4$ transition (filled circle) fell on the $E2$ curve. Solid lines are theoretical curves from Ref. 22. The point at 438 keV represents a mixture of the $12_\beta \rightarrow 12$ and $10_\beta \rightarrow 8_\beta$ transitions.

$12_\beta \rightarrow 12$ transition, a value which is comparable to that for the other $I_\beta \rightarrow I$ transitions and which implies a substantial $E0$ admixture in the $12_\beta \rightarrow 12$ transition.

Transition intensities from spin states above 12 could not be obtained from the present electron spectra. The transition energy for the $14_\beta \rightarrow 14$ transition is 249.8 keV. The electron lines from this weak transition are obscured by the lines from the much stronger $4 \rightarrow 2$ ground-band transition (247.8 keV). By spin 16 the electron energy is too low for conversion electrons to be observed on the present electron spectrometer.

IV. DISCUSSION

The $E0$ transition probability is given by

$$W(E0) = \rho^2 \Omega_K, \quad (6)$$

where ρ is the nuclear $E0$ matrix element and Ω_K is a factor determined by electron wave functions; values of the latter function are given in Refs. 25 and 26. For a deformed nucleus with a uniform charge distribution, Rasmussen²⁷ has introduced a dimensionless quantity X to describe the ratio of transition probabilities, $E0$ to $E2$, for depopulating the band head of a β band. This ratio is given by

$$X(0_\beta \rightarrow 0) = \frac{\rho^2 e^2 R_0^4}{B(E2; 0_\beta \rightarrow 2)} = 4\beta_0^2. \quad (7)$$

Here R_0 is the undeformed nuclear radius given by $1.20A^{1/3}$ fm and β_0 is the deformation parameter. For transitions other than from the β band head, the ratio is generalized²⁸ to

$$X(I_\beta \rightarrow I) = \frac{\rho^2 e^2 R_0^4}{B(E2; I_\beta \rightarrow I)}, \quad (8)$$

where it is understood that $I_\beta = I \neq 0$.

An equivalent form of X which is directly related to experimental quantities is²⁸

$$X = 2.53(\mu_K E_\gamma^5 A^{4/3} / \Omega_K) \times 10^9 \quad (9)$$

in which the transition energy E_γ is in MeV. The quantity μ_K is the ratio of the $E0$ part of the K -conversion-electron intensity to the $E2$ γ -ray intensity. Experimentally μ_K is evaluated from

$$\mu_K = \delta^{-2} [\alpha_K(\text{exp}) - \alpha_K(M1)] + [\alpha_K(\text{exp}) - \alpha_K(E2)]. \quad (10)$$

The quantity δ is the $E2/M1$ mixing ratio. Values of δ used in this work have been taken from γ -ray directional correlation studies in radioactive decay¹³ and from γ -ray angular distributions observed in $(\alpha, n\gamma)$ reactions.^{3,15} These literature values are summarized in Table II. The more precise

TABLE II. Mixing ratio δ and X values for $I_\beta \rightarrow I$ transitions in ^{154}Gd .

Transition	$\delta(E2/M1)$	$X(I_\beta \rightarrow I)$		
		This work	Rud ^a	Riedinger ^b
$(0_\beta \rightarrow 0)/(0_\beta \rightarrow 2)$			0.067 ± 0.011	0.11 ± 0.03
$2_\beta \rightarrow 2$	-10_{-11}^{+4} ^a		0.362 ± 0.012	0.45 ± 0.04
$4_\beta \rightarrow 4$	-7_{-3}^{+2} ^a	0.34 ± 0.07	0.34 ± 0.05	0.58 ± 0.18
$6_\beta \rightarrow 6$	$3.5_{-2.0}^{+2.5}$, ^c $1.8_{-0.2}^{+0.3}$ ^d	0.34 ± 0.08	0.40 ± 0.12	
$8_\beta \rightarrow 8$	$1.0_{-0.6}^{+0.7}$, ^c $1.2_{-0.3}^{+0.4}$ ^d	$0.48_{-0.11}^{+0.18}$		
$10_\beta \rightarrow 10$	$1.1_{-0.3}^{+0.5}$ ^d	$0.27_{-0.12}^{+0.18}$		

^a Reference 12.^b Reference 13.^c Reference 15.^d Based on A_2/A_0 values from Ref. 3; sign chosen to agree with Ref. 15.

values of Ref. 3 have been used in this work.

Values for the ratio X as deduced from the data of this experiment and values reported in earlier experiments^{12,13} are listed in Table II. Where the data overlap, the agreement is generally adequate. The relatively large error for the states of spin 8 and 10 arises chiefly from the uncertainty in δ .

Figure 5 shows that there is a large $E0$ component in the interband transitions up to at least spin 10 and probably also spin 12. This implies that the β -vibrational character is retained in the band up to at least the 10_β state. To investigate how the experimental $E0/E2$ ratio depends on spin from an intrinsic point of view, we remove the geometrical factor from the $B(E2)$ term in the denominator in Eq. (8). We define a reduced quantity X_0 as

$$X_0 \equiv X(I_\beta \rightarrow I) \langle I_\beta 200 | I 0 \rangle^2 = \frac{\rho^2 e^2 R_0^4}{\langle \chi | \mathfrak{M}'(E2) | \chi_\beta \rangle^2}, \quad (11)$$

where χ is the intrinsic part of the wave function in a rotational model.

In Fig. 6 we plot X_0 values as a function of I_β . Within experimental error, X_0 appears to be constant for I_β in the range 2 to 8. Two sets of data^{12,13} indicate that X_0 increases as I_β increases from 0 to 2. The point at $I_\beta = 10$ suggests a decreasing tendency in X_0 but the error is too large to make a definitive statement.

The rise in X_0 at low spin has been explained by Rud *et al.*^{12,16} as resulting from band mixing among ground, β , and γ bands which reduces the $E2$ strength. They have shown that ρ is independent of I , at least to spin 6.

In the adiabatic rotor model, both the numerator and denominator of Eq. (11) should remain constant; thus the constancy of X_0 is not surprising. At higher spin, however, deviations are expected.

If the band-mixing approach of Rud *et al.*¹² is extended to higher spin with their mixing parameters, X_0 is predicted to be about 0.4 for $I_\beta = 10$. Since the first-order perturbation method used by Rud *et al.*¹² is not expected to be reliable at higher spin, the lack of agreement is not surprising.

The present data are examined in context of the intersecting-band hypothesis.⁴⁻⁶ Broglia *et al.*²⁹ have recently presented a model in which three bands (ground, β , and a $K = 1$ band) are mixed. They are able to account for the backbending observed in the ground and β bands of ^{154}Gd . They assume that the only nonzero unperturbed matrix elements are equal to each other and given by

$$\begin{aligned} \langle g | \mathfrak{M}'(E2) | g \rangle &= \langle \beta | \mathfrak{M}'(E2) | \beta \rangle \\ &= \langle \beta | \mathfrak{M}'(E2) | g \rangle = \left(\frac{5}{16}\pi\right)^{1/2} Q_0; \end{aligned} \quad (12)$$

all other matrix elements are disregarded. With this choice of matrix elements they obtain reason-

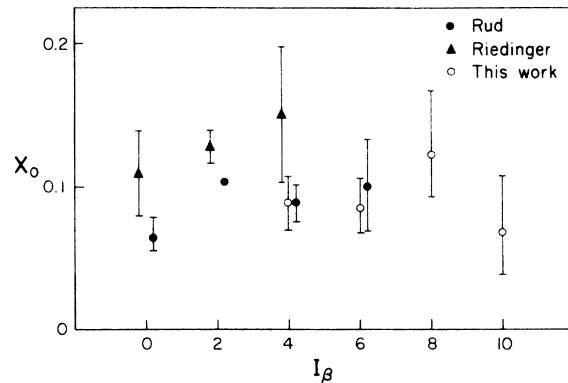


FIG. 6. The parameter X_0 [see Eq. (11)] as a function of I_β . Open circles represent data from the present work, filled circles from Ref. 12, and triangles from Ref. 13.

able agreement with experimental⁴ $E2$ transition probabilities for high-spin states.

To evaluate our experimental results in context of this model, we must make some assumptions about unperturbed $E0$ matrix elements. The leading-order terms for the diagonal matrix elements of the $E0$ operator $\mathfrak{M}'(E0)$ are equal and given by the value for a uniformly charged spherical nucleus. That is,

$$\begin{aligned} \langle g | \mathfrak{M}'(E0) | g \rangle &= \langle \beta | \mathfrak{M}'(E0) | \beta \rangle \\ &= \langle K=1 | \mathfrak{M}'(E0) | K=1 \rangle = \frac{3}{5} Z. \end{aligned} \quad (13)$$

The off-diagonal matrix element is proportional to the zero-point amplitude of the β vibration²⁷ and should be much smaller than the diagonal matrix elements. Formally we write [cf. Eq. (6)]

$$\langle \beta | \mathfrak{M}'(E0) | g \rangle = \rho. \quad (14)$$

Here the $E0$ operator is given by²⁵

$$\mathfrak{M}'(E0) = \left(\sum_p r_p^2 \right) R_0^{-2}, \quad (15)$$

where the summation is over the Z protons in the nucleus. Together with the $E2$ matrix elements of Broglia *et al.* [Eq. (12)] we have calculated X_0 values as a function of I_β . We note that the value of X_0 does not depend on the magnitude of the diagonal $E0$ matrix elements [Eq. (13)], but only on the assumption that they are equal. We find that X_0 increases with I_β . If we normalize the calculated value of X_0 to the experimental value of 0.1 at $I_\beta = 2$, the calculated X_0 is 0.35 at $I_\beta = 10$, a value much larger than the experimental result.

If we assume that in addition to the $E2$ matrix elements in Eq. (12) the remaining diagonal matrix

$$\langle K=1 | \mathfrak{M}'(E2) | K=1 \rangle = \left(\frac{5}{16} \pi \right)^{1/2} Q_0, \quad (16)$$

then X_0 is independent of I_β , in agreement with experiment. With this assumption, however, the experimental $E2$ branching ratios in the band-crossing region of $I = 16-18$ are no longer reproduced. It does not seem possible with the model of Broglia *et al.* to account for both the present data and those of Ref. 4.

Unfortunately the present results do not extend beyond the backbending region. If the intersecting band arises from a coherently unpaired Mottel-

son-Valatin type state, as suggested in Ref. 4, X_0 is expected to increase sharply at the phase transition.¹¹ We see no evidence for such a strong effect.

In a microscopic treatment of nuclear rotations at high spins, Kumar³⁰ has shown that the charge isomer shift, $\Delta \langle r^2 \rangle / \langle r^2 \rangle$, should increase with spin for the nucleus ¹⁶⁰Dy up to spin 16 and then decrease to negative values. Backbending occurs at $I = 16-18$ in the ground band of ¹⁶⁰Dy. Furthermore, according to this calculation, the intrinsic quadrupole moment increases by 11% from $I = 0-16$ but decreases by 8% in going from 16 to 18. Since the nuclear charge distribution and the quadrupole moment are directly related to the experimental quantities we have measured, we consider whether the effects predicted by Kumar can be observed in the present experimental data.

According to Kishimoto³¹ the relationship between X_0 and the isomer shift is given by

$$X_0 = 4\beta_0^2 + (16\pi/5)(\Delta \langle r^2 \rangle / \langle r^2 \rangle). \quad (17)$$

In deriving this equation, he uses a band-mixing perturbation approach; the dependence of $E0$ and $E2$ transition moments on stretching/antistretching is calculated from a collective model with the β degree of freedom. Such a treatment is valid only for relatively low spin (e.g., $I \leq 8$), but the general trend in X_0 is expected to be correct. The magnitude of the $4\beta_0^2$ term is determined experimentally at low spin to be about 0.1. Since $\Delta \langle r^2 \rangle / \langle r^2 \rangle$ is typically of the order 10^{-4} , X_0 is an insensitive function of the isomer shift and even a large change in the isomer shift, such as that predicted by Kumar,³⁰ is not likely to be observed in X_0 .

ACKNOWLEDGMENTS

We are indebted to D. R. Zolnowski, D. R. Haenni, M. B. Hughes, and M. D. Devous for their assistance in collecting and analyzing data. We are especially grateful to T. Kishimoto for many discussions about this paper and for permission to refer to his unpublished work. We thank K. Kumar, T. Udagawa, and D. Ward for their advice and suggestions and R. L. Watson for his help in developing the in-beam conversion-electron spectrometer.

† Work supported in part by the Robert A. Welch Foundation and the U. S. Atomic Energy Commission.

¹A. Johnson and Z. Szymanski, *Phys. Rep.* **7**, 181 (1973).

²R. A. Sorensen, *Rev. Mod. Phys.* **45**, 353 (1973).

³D. Ward, R. L. Graham, J. S. Geiger, and H. R.

Andrews, *Phys. Lett.* **44B**, 39 (1973); and private

communication.

⁴T. L. Khoo, F. M. Bernthal, J. S. Boyno, and R. A. Warner, *Phys. Rev. Lett.* **31**, 1146 (1973).

⁵H. R. Andrews, D. Ward, R. L. Graham, and J. S. Geiger, *Nucl. Phys.* **A219**, 141 (1974).

⁶R. M. Lieder, H. Beuscher, W. F. Davidson,

- A. Neskakis, C. Mayer-Böricke, Y. El. Masri, J. Steyaert, and J. Vervier, *Phys. Lett.* **49B**, 161 (1974).
- ⁷B. R. Mottelson and J. G. Valatin, *Phys. Rev. Lett.* **5**, 511 (1960).
- ⁸J. Krumlinde and Z. Szymanski, *Phys. Lett.* **36B**, 157 (1971).
- ⁹F. S. Stephens and R. S. Simon, *Nucl. Phys.* **A183**, 257 (1972).
- ¹⁰A. Molinari and T. Regge, *Phys. Lett.* **41B**, 93 (1972).
- ¹¹K. Kumar, private communication.
- ¹²N. Rud, H. L. Neilsen, and K. Wilsky, *Nucl. Phys.* **A167**, 401 (1971).
- ¹³L. L. Riedinger, N. R. Johnson, and J. H. Hamilton, *Phys. Rev.* **179**, 1214 (1969).
- ¹⁴O. Lönsjö and G. B. Hagemann, *Nucl. Phys.* **88**, 624 (1966).
- ¹⁵H. Ejiri, S. M. Ferguson, and R. Heffner, Annual Report, Nuclear Physics Laboratory, University of Washington, 1970 (unpublished).
- ¹⁶N. Rud, G. T. Ewan, A. Christy, D. Ward, R. L. Graham, and J. S. Geiger, *Nucl. Phys.* **A191**, 545 (1972).
- ¹⁷R. L. Watson, J. O. Rasmussen, and H. R. Bowman, *Rev. Sci. Instrum.* **38**, 105 (1967).
- ¹⁸C. J. Allan, *Nucl. Instrum. Methods* **91**, 117 (1971).
- ¹⁹E. P. Grigorev, A. V. Zolotavin, V. Ya. Klementev, and R. V. Sinitsyn, *Nucl. Phys.* **14**, 443 (1960).
- ²⁰C. M. Lederer, J. M. Hollander, and I. Perlman, *Table of Isotopes* (Wiley, New York, 1967), 6th ed.
- ²¹Y. Gono, to be published.
- ²²R. S. Hager and E. C. Seltzer, *Nucl. Data* **A4**, 1 (1968).
- ²³R. S. Hager and E. C. Seltzer, *Nucl. Data* **A4**, 397 (1968).
- ²⁴K. Siegbahn, in *Alpha-, Beta-, and Gamma-Ray Spectroscopy*, edited by K. Siegbahn (North-Holland, Amsterdam, 1967), p. 142.
- ²⁵E. L. Church and J. Weneser, *Phys. Rev.* **103**, 1035 (1956); *Annu. Rev. Nucl. Sci.* **10**, 193 (1960).
- ²⁶D. A. Bell, C. A. Avoledo, M. G. Davidson, and J. P. Davidson, *Can. J. Phys.* **48**, 2542 (1970).
- ²⁷J. O. Rasmussen, *Nucl. Phys.* **19**, 85 (1960).
- ²⁸J. P. Davidson, *Nucl. Phys.* **86**, 561 (1966).
- ²⁹R. A. Broglia, A. Molinari, G. Pollarolo, and T. Regge, *Phys. Lett.* **50B**, 295 (1974).
- ³⁰K. Kumar, *Phys. Rev. Lett.* **30**, 1227 (1973).
- ³¹T. Kishimoto, private communication.